

Journal of
Mechanics of
Materials and Structures

**STATISTICS OF MICROSTRUCTURE, PEAK STRESS AND
INTERFACE DAMAGE IN FIBER REINFORCED COMPOSITES**

Volodymyr I. Kushch, Sergii V. Shmegeera and Leon Mishnaevsky Jr.

Volume 4, N° 6

June 2009



mathematical sciences publishers

STATISTICS OF MICROSTRUCTURE, PEAK STRESS AND INTERFACE DAMAGE IN FIBER REINFORCED COMPOSITES

VOLODYMYR I. KUSHCH, SERGII V. SHMEGERA AND LEON MISHNAEVSKY JR.

This paper addresses an effect of the fiber arrangement and interactions on the peak interface stress statistics in a fiber reinforced composite material (FRC). The method we apply combines the multipole expansion technique with the representative unit cell model of composite bulk, which is able to simulate both the uniform and clustered random fiber arrangements. By averaging over a number of numerical tests, the empirical probability functions have been obtained for the nearest neighbor distance and the peak interface stress. It is shown that the considered statistical parameters are rather sensitive to the fiber arrangement, particularly cluster formation. An explicit correspondence between them has been established and an analytical formula linking the microstructure and peak stress statistics in FRCs has been suggested. Application of the statistical theory of extreme values to the local stress concentration study has been discussed. It is shown that the peak interface stress distribution in the fibrous composite with uniform random microstructure follows a Fréchet-type asymptotic distribution rule. Based on the established statistical distributions, a simple microdamage model of FRC is suggested.

1. Introduction

A quantitative analysis of an effect caused by the distribution of inhomogeneities in a heterogeneous material on its local and overall mechanical behavior is one of the most challenging problems of the micromechanics of composites. This problem stems from the actual needs of materials science since random microstructure is inherent for most heterogeneous materials including fiber reinforced composites (FRCs). The complexity in formulating the FRC strength theory arises from the fact that the strength limit/fracture onset is governed by the maximum local stress rather than by its mean value. Except in the very dilute case, interaction between the fibers results in stress concentration on them which deviates from that observed for a single fiber embedded in an unbounded matrix and, due to the randomness of the structure of the composite, is a random function of spatial coordinates. The peak stress location and level are rather sensitive to the arrangement type of the fibers and, therefore, their reliable prediction requires an adequate account of microstructure statistics of actual FRCs and interactions between the fibers. This problem becomes even tougher when the local stress concentration in composites with statistically nonuniform fiber distribution is considered. The difficulty associated with a quantitative description of this effect comes from the fact that the ergodic hypothesis does not hold for the materials with nonuniform microstructure and, therefore, ensemble averaging cannot be replaced by volume averaging and substantial statistical analysis is required (see, for example, [Beran 1968; Torquato 2002]).

A promising way to account for fiber arrangement statistics and interactions between fibers is known in the mechanics of composites as *regularization*, or *representative unit cell* approach (see, for example, [Golovchan et al. 1993; Byström 2003; Drago and Pindera 2007]). It is based on modeling the structure

of an actual heterogeneous solid by a periodic medium whose representative unit cell contains a number of inhomogeneities. This approach appears to be advantageous in that the quasirandom microstructure of such a material, with prescribed statistical structure parameters, can be specified explicitly. Moreover, due to the deterministic nature of this model, it is possible to formulate and solve the periodic model problem accurately and thereby to account for the interactions among the inclusions in a rigorous manner. Below, we refer to a few publications, most relevant to the problem under study, where the above mentioned approach was applied.

The papers [Pyrz 1994a; 1994b; Pyrz and Bochenek 1998] address the problems encountered in the quantitative description of arrangements and correlations in unidirectional fiber reinforced composite materials. It has been indicated there that both topological and second-order statistics are related to the local stress variability under transverse loading conditions. Particular attention was paid to the variability of interfacial maximal radial stresses, and the conclusion was made that peak radial stresses increase with a decrease in the space between fibers. However, the stress analysis performed there must be considered as rather qualitative because the iterative model method they applied is based on superposition of Eshelby's solutions and thus assumes constancy of stress inside the fiber. This assumption may be acceptable for the mean stress evaluation in a weakly heterogeneous material; however, a peak local stress even in the two-fiber problem (see [Buryachenko and Kushch 2006], for example) cannot be captured this way. As shown in [Ganguly and Poole 2004] by comparison with numerical solutions, the iterative model can only be applied to dilute composites with widely separated fibers; more exactly, it is limited to distributions where the minimum interfiber distance exceeds the fiber radius three or more times. To account for interactions between the closely-placed fibers typical of FRC microstructure, an accurate analytical or numerical method should be applied.

In [Babuška et al. 1999], an analysis is focused on the stochastic constitutive properties and statistics of the peak local fiber-matrix interface stresses. For this purpose, a file of the fibers' location and diameter was generated by processing the digitized micrograph of the composite plate cut and, these data were used to formulate the structure model and boundary-value problem. The traction boundary conditions at the cell sides were taken into account by means of a superframe. The numerical method used to solve for stress is the p -version of the finite element method combined with the homogenization procedure. The authors have obtained descriptive statistics of peak interface stresses in FRCs and have shown that actual distribution of fibers produces only a minor effect on the overall elastic properties of the composite.

Chen and Papathanasiou [2004] have used a parallel many-processor implementation of the boundary element method to study the peak stresses in an FRC using a model containing 144 fibers randomly placed inside the square matrix domain. The cell geometry was generated using a Monte Carlo algorithm, controlling the minimum allowable interfiber and fiber-cell side spacing. The resulting interface stresses were found to follow a Weibull-like distribution and the conclusion was reached that the key structure parameter affecting the interface stresses is the distance between the fibers.

In [Kushch et al. 2008] we developed an efficient, multipole expansion technique-based method and numerical code for evaluating the microstress field in a fibrous composite. The method combines the superposition principle, the theory of complex potentials, and Fourier series expansion, in order to reduce the meso cell model problem to an ordinary, well-posed set of linear algebraic equations. By averaging over a number of random structure realizations, statistically meaningful results have been obtained for both the local stress and effective elastic moduli of disordered fibrous composites. It was found, in

particular, that the peak interface stress distribution is fitted well by Gumbel-type statistics of extreme values.

In the present paper, the method of [Kushch et al. 2008] is applied to study the relationship between the fiber arrangement type and the local peak interface stress statistics in FRCs. To this end, the representative unit cell model of fibrous composites capable of simulating both the uniform and clustered random fiber arrangements is used. A series of computational experiments has been carried out and the empirical probability functions have been obtained for the nearest neighbor distance and the peak interface stress. It is shown that the statistical parameters considered are rather sensitive to the fiber arrangement, particularly cluster formation. An explicit correspondence between them is established and the relevant analytical formulas are written. Application of the statistics of extremes to the local stress concentration study is discussed and the conclusion is reached that, with a high degree of probability, the peak interface stress distribution in FRCs with uniform random arrangement of fibers follows the Fréchet rule. Based on the established statistical distributions of local peak stress, a simple microdamage model of FRCs has been suggested.

2. Representative cell model of random structure FRCs

2.1. Model geometry. It was already pointed out in the Introduction that reliable prediction of FRC damage onset and accumulation requires the use of a geometric model statistically close to the microstructure of an actual FRC and an adequate account for interactions between the fibers. This, in turn, necessitates a statistical description of both the geometry and local stress field because random microstructure is inherent for the most FRCs (and hence the stress field appears to be a random function of spatial coordinates as well). On the other hand, the local damage level and strength limit of an FRC is governed by the peak local stress level (rather than its mean value) and location, which is quite sensitive to the fiber arrangement. Therefore, using the probability theory formalism seems to be an adequate, and probably the only consistent, way of linking the statistical parameters of microstructure and peak local stress distribution.

To meet these requirements, we use the many-fiber two-dimensional unit cell model of the FRC bulk, shown in Figure 1. Specifically, we consider a quasirandom, or generalized periodic, model structure (as in [Golovchan et al. 1993; Byström 2003], among others) with the periods a and b along the axes Ox_1 and Ox_2 , respectively, a unit cell of which contains a certain number of fibers of radius R , aligned in the x_3 direction and circular in cross-section. Within a cell, the fibers can be placed arbitrarily but without overlapping. A geometry of the unit cell is given by its length a and height b and the coordinates (X_{1q}, X_{2q}) of the centers of inclusions O_q , $q = 1, 2, \dots, N$. The whole composite bulk can be obtained by translating the cell in two orthogonal directions. Besides the global Cartesian coordinate system Ox_1x_2 , we introduce the local, inclusion-related coordinate systems $Ox_{1q}x_{2q}$ with origins in O_q . Also, we will use the complex-valued variables

$$z = x_1 + ix_2, \quad z_q = x_{1q} + ix_{2q}, \quad (1)$$

representing the point $x = (x_1, x_2)^T$ in the complex planes Ox_1x_2 and $Ox_{1q}x_{2q}$, respectively. Clearly, $z = z_q + Z_q$, where $Z_q = X_{1q} + iX_{2q}$. The number N of fibers with centers inside the cell can be taken to be sufficiently large to approach the microstructure of an actual disordered composite.

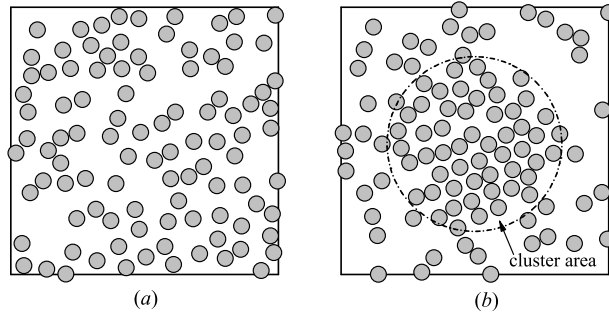


Figure 1. Unit cell model of the FRC bulk with (a) uniform and (b) clustered microstructure.

To generate the quasirandom structure shown in [Figure 1](#), the molecular dynamics algorithm of growing particles is used. An idea of the algorithm is as follows: we start with a certain prescribed number of tiny fibers whose initial positions within a cell and initial velocities are given by the random number generator. Then, the fibers move toward each other, collide elastically, and grow steadily during a period of $1000N$ collisions. In the case any fiber (more exactly, its center) traversed the cell boundary, it enters the cell from the opposite side. It preserves both the fiber volume content and periodicity of structure. After the volume content of fibers reached the prescribed value, the system is further equilibrated for a period of $5000N$ collisions, sufficient to guarantee reproducible thermodynamic properties of the model [\[Torquato 2002\]](#).

The geometry considered can be characterized by several parameters, including the fiber volume content $c = N\pi R^2/ab$, coordination number, second-order intensity function, radial distribution function, etc. (see, for example, [\[Pyrz 1994b; Buryachenko et al. 2003\]](#)). The structure parameters we focus on are the normalized nearest-neighbor distance,

$$d_m = \min_{p \neq q} |Z_{pq}| / D,$$

and interfiber spacing $\delta = d_m - 1$, where $Z_{pq} = Z_p - Z_q$ defines the relative position of the fibers and $D = 2R$ is the diameter of a fiber. In the many-fiber models of FRC, the “minimum allowable interfiber spacing” parameter δ^* [\[Chen and Papathanasiou 2004\]](#) is often introduced so that any two fibers are effectively separated: $\delta \geq \delta^* > 0$. It is also known as the impenetrability parameter, in terms of the cherry-pit model [\[Torquato 2002\]](#). Obviously, the smaller δ^* is, the stiffer the model boundary value problem is (no matter what analytical or numerical method we apply to solve it), and the higher the expected local stress concentration is. By prescribing a fixed allowable spacing δ^* , we, in fact, predetermine the maximum allowable stress; and, to be consistent with practice, this parameter should be taken to be as small as possible. Some idea of how the stress concentration is affected by δ can be gotten from the stress asymptotes for nearly touching fibers. Note that the stress remains finite when the fibers are drawn together ($\delta \rightarrow 0$; see [Figure 2](#)): the stress singularity is expected only in the case of rigid (nondeformable) fibers. A small positive value is usually assigned to this parameter in order to separate fibers and thus alleviate either analytical or numerical analysis of the boundary value problem. In the present study, $\delta^* = 0.01$ is taken. Variation of this parameter slightly influences the absolute value of the local stress concentrations, but does not change the qualitative behavior of the local and averaged fields.

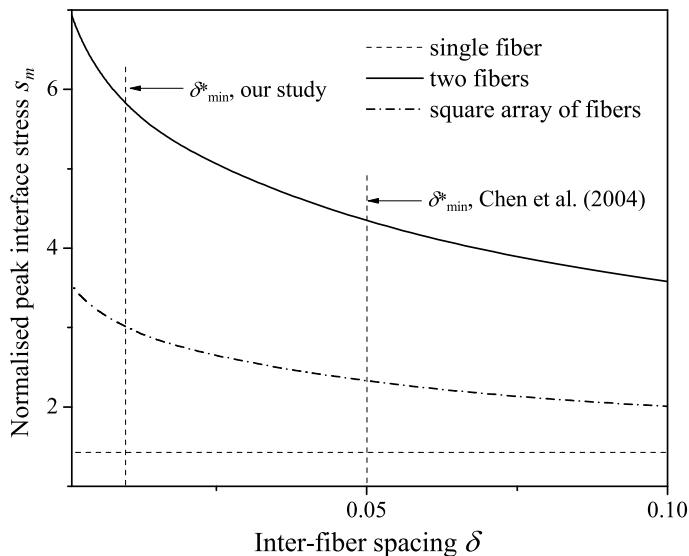


Figure 2. Interface stress concentration as a function of interfiber spacing.

The model we consider is sufficiently flexible to also simulate a composite with nonuniform distribution of fibers. Specifically, we consider the cluster of fibers of circular shape shown in Figure 1(b): its size is defined by the radius R_{cl} or, alternatively, by the volume content of clusters $c_{cl} = \pi R_{cl}^2/ab$. Due to presence in this model of an additional structure parameter, the cluster radius $R_{cl} \gg R$, it can be thought of as a meso level model; for more discussion on the subject, see [Mishnaevsky 2007]. It can be obtained in the following way: first, the uniform microstructure is generated as described above, with the fiber volume content c_{in} equal to that inside the cluster. The fibers outside the cluster are then removed randomly, one by one, until the prescribed overall volume content c is reached. A drawback of this simple method is that the random elimination procedure may lead to the percolation type structure. In principle, it is possible to fix this problem by applying the previously described “equilibration” procedure to the area outside the cluster. In our numerical study, the fiber volume content outside the cluster c_{out} is sufficiently low and we expect the mentioned nonuniformity of the microstructure to produce a minor effect on the statistics of elastic fields.

2.2. Model problem. By adopting a two-dimensional model, we assume $\partial\sigma_{ij}/\partial x_3 = 0$: within this framework, the plane strain, plane stress and antiplane shear (in the x_3 -direction) problems can be studied. Specifically, we consider the plane strain problem ($u_3 = 0$) as a consequence, and $\epsilon_{33} = \epsilon_{13} = \epsilon_{23} = 0$ as well. Both the matrix and fiber materials are isotropic and linearly elastic.

We denote by $u_m = u_{m1} + iu_{m2}$ the displacement in a matrix material with a shear modulus G_0 and Poisson ratio ν_0 ; $u_i^{(q)}$, G_q , and ν_q refer to displacement and elastic moduli, respectively, of the q th fiber, $q = 1, 2, \dots, N$. Here, u_i are the Cartesian components of the displacement vector $u = (u_1, u_2)^T$. At the matrix-fiber interfaces, perfect bonding conditions are prescribed:

$$(u_m - u_i^{(q)})|_{|z_q|=R} = 0, \quad (\tau_n(u_m) - \tau_n(u_i^{(q)}))|_{|z_q|=R} = 0, \quad q = 1, 2, \dots, N, \quad (2)$$

where $\tau_n = \sigma_{rr} + i\sigma_{r\varphi}$.

The stress field in the composite bulk is assumed to be macroscopically homogeneous, which means constancy of the volume-averaged, or macroscopic, strain $\varepsilon^* = \{\varepsilon_{ij}^*\} = \{\langle \varepsilon_{ij} \rangle\}$ and stress $\sigma^* = \{\sigma_{ij}^*\} = \{\langle \sigma_{ij} \rangle\}$ tensors, where $\langle f \rangle = \int_V f dV$ and V is the cell volume; in our case, $V = ab$.

In the problem we consider, the far field load can be defined either by the macroscopic strain tensor ε^* , or by the macroscopic stress tensor σ^* . The first case is typical in the homogenization problem where the macroscopic, or effective, moduli are of the primary interest. On the other hand, using the macrostress tensor σ^* as a load governing parameter is preferable in the local stress concentration study. Next, it is common knowledge that under macroscopic stress homogeneity conditions, periodicity of structure results in periodicity of relevant physical fields. In our case, the periodicity condition

$$\sigma_{ij}(z+a) = \sigma_{ij}(z+ib) = \sigma_{ij}(z) \quad (3)$$

can be alternatively regarded as the cell boundary condition providing continuity of the displacement and stress fields between the adjacent cells.

2.3. Numerical method and implementation. It should be clearly understood that a one-time solution of the model problem for a specific realization of quasirandom geometry shown in [Figure 1](#) is not sufficient for our purpose, even if it is highly accurate. A convergent and statistically valid solution requires a sufficiently large number of numerical tests N_{test} to be conducted, with subsequent averaging the numerical data obtained. In this situation, the efficiency of the method we apply to solve for stress is of critical importance. It appears that a total computational cost of the direct numerical (finite element and boundary element) methods is exceedingly large. A preferable choice is the multipole expansion-based technique (see [[Greengard and Helsing 1998](#); [Wang et al. 2005](#)], for example), which provides fast and accurate solutions for the problems of this kind. The theory and numerical algorithm of the method we apply in this work is exposed in [[Kushch et al. 2008](#)]. Here, we note only that this method combines the superposition principle, the theory of complex potentials, and the Fourier series technique to give an asymptotically exact solution. This means that, in order to get the exact values, one must solve an infinite set of linear equations. In practice, it is solved by applying the truncation method where only a finite number N_{eqn} of equations and unknowns is retained in the infinite system. An approximate solution obtained in this way converges to the exact one with $N_{\text{eqn}} \rightarrow \infty$ and, thus, any desirable accuracy can be achieved by the proper choice of N_{eqn} .

Numerical efficiency of the method stems from the fact that the main part of the solution, namely, reduction of the cell model boundary-value problem to a system of linear algebraic equations, is done analytically. The matrix coefficients of this system are given by simple rational expressions and, unlike in the direct numerical schemes, involve no integration. Instead, they contain the absolutely convergent ordinary sums which can be calculated in advance. In fact, the most computation time is spent by the linear solver and, to provide high performance, the generalized minimum residuals (GMRES) algorithm of [[Saad and Schultz 1986](#)] with a block-Jacobi preconditioner is applied. In our numerical study we used open source GMRES code in Fortran [[Frayssse et al. 1998](#)], with minor modifications. All the below reported numerical data correspond to the uniaxial tension $\sigma_{22}^* = P$ of a model FRC ([Figure 1](#)). The following elastic properties of the components of the composite are taken: $E_0 = 3.2$ GPa and $\nu_0 = 0.36$ for the matrix; $E_p = 70.6$ GPa and $\nu_p = 0.25$ for fibers [[Meraghni et al. 2002](#)].

Three main parameters governing convergence and accuracy of the below performed statistical study are the number N_{fib} of fibers with the centers inside the unit cell, the number N_{harm} of harmonics retained in the series expansion of local field, and the number N_{test} of the random structure realizations taken for averaging. Obviously, all these numbers should be taken to be sufficiently large to provide reliable numerical results. On the other hand, a total computational effort of this study scales as $(N_{\text{eqn}})^2 N_{\text{test}}$, where the number of equations retained in the linear system is $N_{\text{eqn}} = 2N_{\text{fib}}N_{\text{harm}}$. To minimize computational time, the appropriate numbers N_{harm} , N_{fib} and N_{test} should be taken. Their choice is based on the convergence study of [Kushch et al. 2008]; in the subsequent numerical study, we take $N_{\text{harm}} = 20$, $N_{\text{fib}} = 100$ and $N_{\text{test}} = 50$. In our numerical experiments, we put $a = b = R\sqrt{\pi N_{\text{fib}}/c}$.

3. Peak interface stress in FRCs

3.1. Deterministic models. Now, we proceed with analysis of the local stress field in a FRC. Specifically, we study an effect caused by the fiber arrangement type on the interface stress concentration, or normalized peak stress,

$$s_m = \max_{0 \leq \varphi < 2\pi} \sigma_{rr} / P.$$

Assuming this stress is responsible for the damage (say, interface crack) onset, one can think of the “interface strength” affected by microstructure. Sometimes [Degrieck and van Paepegem 2001; Foster et al. 2006], the debonding criterion is taken in more general form

$$(\sigma_{rr})^2 + \beta(\sigma_{r\varphi})^2 = \text{const},$$

which, however, does not alter the way of the structure-strength relationship study. And, although we restrict ourselves to considering the uniaxial tension $\sigma_{22}^* = P$, the extension to the complex macrostress state is rather straightforward since the theory we use is valid for an arbitrary loading type.

In the case of periodic arrangement of fibers, one-to-one functional relationship between the structure parameters and stress concentration can be established. In Figure 2, the s_m value is shown as a function of normalized nearest neighbor distance in the composite with a square packing of fibers, where $d_m = 2\sqrt{\pi/c}$. An accurate analysis shows that peak interface stress grows as the volume content c of fibers increases. In the dilute case $c \rightarrow 0$ ($d_m \rightarrow \infty$), we have $s_m = 1.426$ (dashed line); the stress concentration between two fibers embedded in an unbounded solid ($Z_{12} = 0 + id_m$) is shown in Figure 2 by the dash-dotted line. As seen from the plot, the two-fiber solution can serve as the upper bound of the peak interface stress $s_m(d)$ in the composite, and the $s_m \approx 7$ observed for two nearly touching fibers is, probably, the maximum interface stress attainable in the composite of arbitrary microstructure for these phase properties and loading type. Note that for $\delta^* = 0.05$, adopted in [Chen and Papathanasiou 2004], the probable s_m underestimation is almost twofold. As for the previously mentioned iterative model used in [Pyrz and Bochenek 1998], its applicability condition is $\delta^* > 0.5$ [Ganguly and Poole 2004], which, as seen from Figure 2, leaves no chance to get the correct numbers for local stress. In the subsequent numerical study, we put $\delta^* = 0.01$, which seems to be a reasonable compromise between accuracy and computational effort.

In the random structure FRCs, one cannot expect a deterministic correlation between the nearest neighbor distance and stress concentration s_m , as they both appear to be random numbers. Their statistical distributions will be analyzed below.

3.2. Peak stress statistics in the random structure FRC. For the ordered sample $s_m^{(q_1)} \leq s_m^{(q_2)} \leq \dots \leq s_m^{(q_N)}$ obtained from the computational experiment, we define the empirical cumulative probability function

$$\widehat{F}(\sigma) = \Pr [s_m^{(q_i)} < \sigma] = (i - 0.5)/N_{\text{fib}}. \tag{4}$$

Here, $s_m^{(q_i)}$ means a normalized peak stress at the interface between matrix and q_i th fiber. To obtain the test-independent data, $s_m^{(q_i)}$ were averaged over 50 runs at a given fiber volume content c . The empirical probability function (4) obtained by computer simulations for c from 0.1 to 0.5 is shown in Figure 3.

Numerical study shows that there always exists (regardless of c) a relatively low fraction of fibers with rather high interface stress. As would be expected, the maximum stress is localized between the closely placed fiber pairs and greatly exceeds the mean stress value. In terms of interface strength, this means that debonding will occur in these “hot spots” much earlier than in the other sites. This observation correlates well with — and can be quite a plausible explanation of — the experimentally observed ([Brøndsted et al. 1997; van Paepegem and Degrieck 2002], among others), rapid FRC stiffness degradation due to matrix-fiber debonding at the initial stage of cyclic loading. Similar data were reported in [Kushch et al. 2008], where an analytical approximation of the peak stress distribution by the generalized “chain-of-bundles” rule $F(\sigma) = \exp(-\exp(-k(\sigma^\alpha - \sigma_c)))$, known also as the generalized Gnedenko–Gumbel distribution [Bolotin 1988] has been suggested. It was shown there that the Weibull’s statistics of peak interface stress claimed in [Chen and Papathanasiou 2004] apply only to the model FRC with well-separated fibers ($\delta_{\text{min}} \geq 0.05$), which considerably underestimates the true interface stress.

3.3. Peak interface stress and statistics of extremes. Thus, an intriguing question arises: is such a close correlation between the peak stress statistics obtained from numerical tests and the known statistical distributions, used by us as the fitting functions, simply a matter of luck? Or is it possibly the manifestation of a certain intrinsic rule? In attempt to answer this question, we refer to the statistical theory

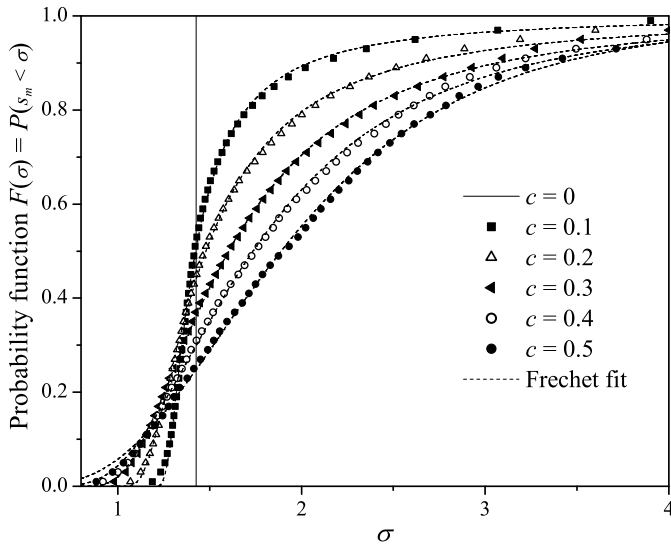


Figure 3. Empirical probability function of the peak interface stress s_m : an effect of fiber volume content.

of extreme values called *statistics of extremes*. This is a modern and rather promising branch of the probability theory [Beirlant et al. 2004]; for a reader unacquainted with the statistics of extremes, a brief introductory note is provided below.

Extreme values theory is concerned with probabilistic and statistical questions related to very high or very low values in sequences of random variables and in stochastic processes. The subject has a rich mathematical theory and applications in a variety of areas. Historically, work on extreme values problems may be traced back to as early as 1709, when N. Bernouilli discussed the mean largest distance $M(\xi)$ from the origin, given N points X_n lying at random on a straight line of a fixed length L : $\xi = \max_n X_n$. The first systematic account of the statistical theory of extremes was done by Gumbel [1958], who studied, in particular, statistics of meteorological phenomena such as snowfalls, wind gusts and river floodings. The typical problem of this class consists in finding the probability $\Pr[\max X_n \geq h]$ where, say, X_n is the river level and h is the dam height. Needless to say, this number is of vital importance because it speaks of the likelihood of catastrophic event. Analogous, practically important problems arise in a variety of areas including natural sciences, military and civil engineering, weather, climate, finances, stock marketing, etc.

The first writer to realize the close connection between specimen strength and distribution of extreme values seems to be F. T. Peirce of the British Cotton Industry Association. The application of essentially the same ideas to the study of the strength of materials was carried out by von Mises and W. Weibull, among others; for more details, see [Freudenthal 1968; Beirlant et al. 2004]. However, Gumbel was the first to call the attention of engineers and statisticians to the possible applications of the formal extreme-value theory to certain distributions which had previously been treated empirically. One of the principal results of this theory is the so-called *Three Types Theorem*, originally stated without mathematical proof in [Fisher and Tippett 1928] and later derived rigorously in [Gnedenko 1943]. It asserts that if a distribution function does not put all its mass at a single point, it must be one of three types:

$$\text{Gumbel type:} \quad G(x) = \Pr[\xi < x] = \exp(-\exp((x - p_1)/p_3)), \quad \text{all } x; \quad (5)$$

$$\text{Fréchet type:} \quad F(x) = \Pr[\xi < x] = \begin{cases} 0 & \text{for } x < p_1, \\ \exp(-(x - p_1)/p_3)^{-p_2} & \text{for } x \geq p_1; \end{cases} \quad (6)$$

$$\text{Weibull type:} \quad W(x) = \Pr[\xi < x] = \begin{cases} \exp(-(p_1 - x)/p_3)^{p_2} & \text{for } x \leq p_1; \\ 1 & \text{for } x > p_1; \end{cases} \quad (7)$$

where p_1, p_2, p_3 are parameters, the last two of which are positive. In fact, this theorem gives a rigorous theoretical substantiation to the already known, empirically found statistical distributions. Importantly, it also says what kind of distribution is expected in that or another case. They differ by shape and, due to their behavior at large x , are sometimes called long-tailed (Fréchet), medium-tailed (Gumbel) and short-tailed (Weibull). The corresponding distributions of $(-\xi)$ are also called extreme value distributions; in this case we come to the Weibull function in its commonly known form:

$$W(x) = 1 - \exp(-((x - p_1)/p_3)^{p_2}) \quad (x > p_1). \quad (8)$$

Now, we come back to our problem and reveal that it also can be thought of in the context of statistics of extremes. We do not claim to have a rigorous proof of the applicability of the Three Types Theorem to the random variable $s_m = \max \sigma_{rr}/P$; rather, we try to check it numerically. For the uniaxial tension

	$c = 0.1$	$c = 0.2$	$c = 0.3$	$c = 0.4$	$c = 0.5$	b_{i0}	b_{i1}	b_{i2}
p_1	1.19	0.939	0.473	-0.265	-2.78	1.246	-0.0441	0.111
p_2	1.45	1.65	2.27	3.29	6.70	1.393	0.0389	0.102
p_3	0.181	0.433	0.962	1.79	4.42	0.128	0.0492	0.112

Table 1. Parameters of the fitting function (8).

$\sigma_{22}^* = P$, the conservative bound for s_m is $s_m > 0$. Thus we consider, at least formally, the Fréchet distribution (6) as a plausible analytical form of the cumulative probability function $F(\sigma) = \Pr\{s_m < \sigma\}$. The values of parameters p_i in (6), found by the least-square fit of the numerical data in Figure 3, are given in Table 1. The negative p_1 (for example, equal to -2.78 for $c = 0.5$) does not cause problems: while compressive s_m is formally allowed in (6), the estimated probability of $(s_m < 0.5)$ is $6.3 \cdot 10^{-4}$ and that of $(s_m < 0)$ about $2 \cdot 10^{-10}$ — that is, an impossible event.

The corresponding best fit curves are shown in Figure 3 by the dashed lines. As seen from the plot, the results of (6) practically coincide with those of the computer simulation, if we take appropriate values for the p_i . An attempt to use the Gumbel distribution (5) as a fitting function (dash-dotted curves in Figure 4) cannot be considered as successful; the discrepancy is significant and peaks in the high stress area, which is the area responsible for strength and therefore the most interesting to us. Finally, the Weibull-type distribution (7) fails completely to approximate the data obtained from numerical experiments; but the fit by the Weibull function (8) is almost as good as that of (6). For $c = 0.1$ the goodness of the fit in terms of reduced χ^2 parameter is equal to $1.5 \cdot 10^{-4}$ for (6), $1.5 \cdot 10^{-3}$ for (8) and $2.7 \cdot 10^{-3}$ for (5); the same tendency exists for higher values of c .

Thus, the conclusion can be drawn that, with a high degree of probability, the peak interface stress distribution in FRCs with uniform random arrangement of fibers follows the Fréchet rule. Using the data from Table 1, one also can find the dependencies $p_i = p_i(c)$. It turns out that all p_i are fitted satisfactorily

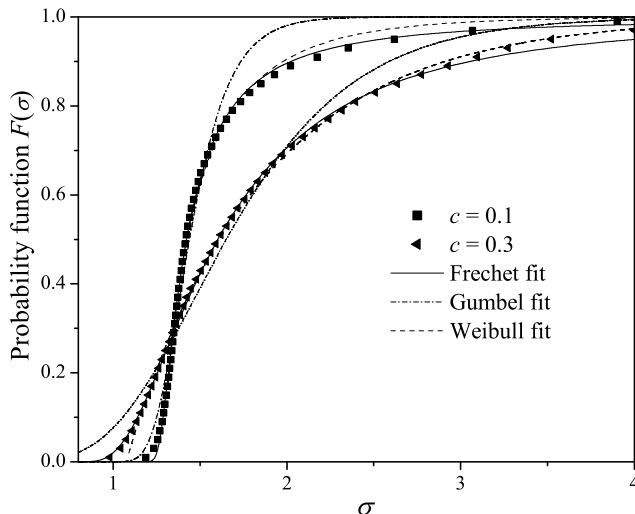


Figure 4. Fréchet, Weibull and Gumbel distributions as fitting functions.

by the function $p_i(c) = b_{i0} + b_{i1} \exp(c/b_{i2})$; the coefficients b_{ij} are given in the last three columns of [Table 1](#). Below, we take $F(\sigma) = \exp(-(p_3(c)/(\sigma - p_1(c)))^{p_2(c)})$ as the analytical form of the probability function $\Pr[s_m < \sigma]$.

4. Correlation between microstructure and peak stress

4.1. Microstructure statistics: nearest neighbor distance. Since stress concentration on a given fiber is greatly amplified by the surrounding fibers, peak stress location and magnitude appear to be rather sensitive to the fiber arrangement type. Therefore, reliable prediction of s_m distribution requires an adequate account for the microstructure statistics of actual FRCs. The most important factors characterizing microstructures of composites are shape, volume fraction, and arrangement of the constituents. The latter, in turn, can be characterized by several parameters, including coordination number, particle cage, interparticle spacing, second-order intensity (Ripley’s) function, radial distribution function, nearest neighbor distribution function, two-point cluster function, etc. (see, for example, [\[Pyrz 1994b; Babuška et al. 1999; Torquato 2002; Buryachenko et al. 2003\]](#)).

At the same time, a very few publications are known to the authors where the relationships between the statistics of structure and local fields were established. The attempts to use the marked correlation function as a link between the geometrical features of a microstructure and stress concentration [\[Pyrz 1994a; 1994b; Pyrz and Bochenek 1998; Chen and Papathanasiou 2004\]](#) cannot be considered convincing. Probably, the most definite (mainly qualitative, however) conclusion drawn there is that s_m amplification and its variability is strongly affected by the nearest neighbor distance and nearest neighbor orientations of adjacent fibers, and therefore the stress amplification is more pronounced for the clustered structure as compared with the statistically uniform one. An important and challenging question arises regarding the $s_m - d_m$ correlation in a FRC with random microstructure.

To answer this question, we use results of [Torquato \[1995\]](#) on nearest neighbor statistics for the packing of hard disks. He introduced the exclusion probability function $E(r)$, equal to the probability that a circular region of radius r encompassing the reference fiber is free of other fiber centers. In our notation, $E(r) = \Pr[d_m > r/D]$. The following analytical representation was found by Torquato:

$$E(r) = \exp(-c(4a_0(r^2/D^2 - 1) + 8a_1(r/D - 1))), \tag{9}$$

where $a_0 = (1 + 0.128c) / (1 - c)^2$ and $a_1 = -0.564c / (1 - c)^2$. To apply these results to our case, we account for the parameter δ^* (minimum interfiber spacing) introduced in [Section 2](#). Specifically, in [\(9\)](#) we use $\tilde{r} = r/(1 + \delta^*)$ and $\tilde{c} = c(1 + \delta^*)^2$ instead of r and c .

[Figure 5](#) compares the results calculated according to [\(9\)](#) with our numerical results on the nearest neighbor statistics. There, the symbols represent the empirical exclusion probability function obtained in the following way. First, for each fiber we find

$$d_m^{(q)} = \min_{p \neq q} |Z_{pq}| / D;$$

next, for the ordered sample $d_m^{(q_1)} \leq d_m^{(q_2)} \leq \dots \leq d_m^{(q_N)}$ we define the empirical cumulative probability function

$$\widehat{E}(r) = \Pr[d_m^{(q_i)} > r/D] = 1 - (i - 0.5)/N_{\text{fib}}. \tag{10}$$

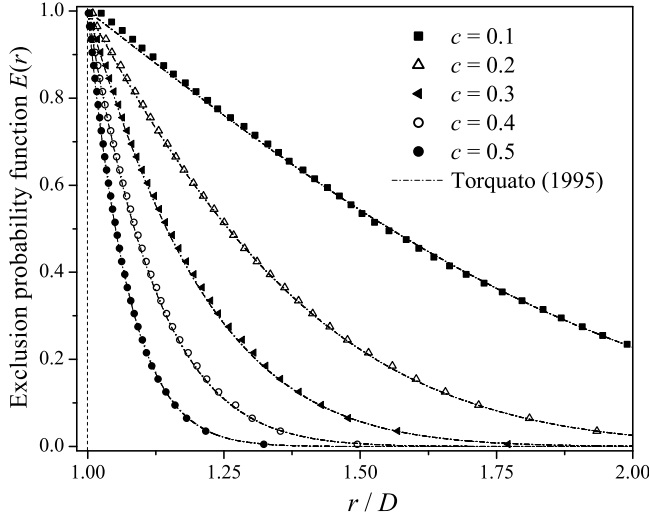


Figure 5. Exclusion probability function: numerical simulation and approximation.

To obtain the test-independent data, $d_m^{(q_i)}$ were averaged over 50 realizations of random structure for a given fiber volume content c . As seen from the plot, the results of the computer simulation are in very close agreement with the theory, which validates the algorithm and computer code used for generation of the cell geometry. Hence, one can use (9) as an analytical characteristic of the statistically uniform random microstructure of FRCs.

4.2. Stress concentration versus nearest neighbor distance. Both s_m and d_m are the random numbers: no direct functional dependence is expected between them. At the same time, such a relationship can be easily found between the arguments of the relevant probability functions, $F(\sigma)$ and $E(r)$. Namely, we equate the probability of finding the neighbor fiber at the distance larger than d_m to the probability that the peak interface stress s_m does not exceed a certain value σ . By combining (9) and (6) we get the explicit formula

$$\sigma(r) = p_1(c) + p_3(c) \left(c(4a_0(r^2/D^2 - 1) + 8a_1(r/D - 1)) \right)^{-1/p_2(c)}. \quad (11)$$

The empirical dependencies $\sigma(r)$ obtained by matching the numerical data in Figures 3 and 5 are shown in Figure 6 by discrete symbols; the dash-dotted lines represent (11). As seen from the plot, agreement between the numerical data and their analytical representation is quite close. The tendency observed in Figure 6 of the peak stress decreasing with the increase of c is to be anticipated: the higher the fiber volume content is, the less room is left for the isolated clusters of a few fibers where the high interface stress concentration is most probable.

Equation (11) deserves a certain criticism because d_m is the leading, but in no way the only, factor affecting s_m . Another important structure parameter is the nearest neighbor orientation [Pyrz and Bochenek 1998] characterized by the angle φ_m between the line connecting the centers of nearest fibers and loading direction. Some idea of correlation between s_m and φ_m can be gotten from Figure 7, where the raw data of computer simulation for $c = 0.4$ are shown. An angular dependence on peak stress is clearly seen: as expected, the highest s_m is observed in the fiber pairs with φ_m close to $\pm\pi/2$. For the sake of

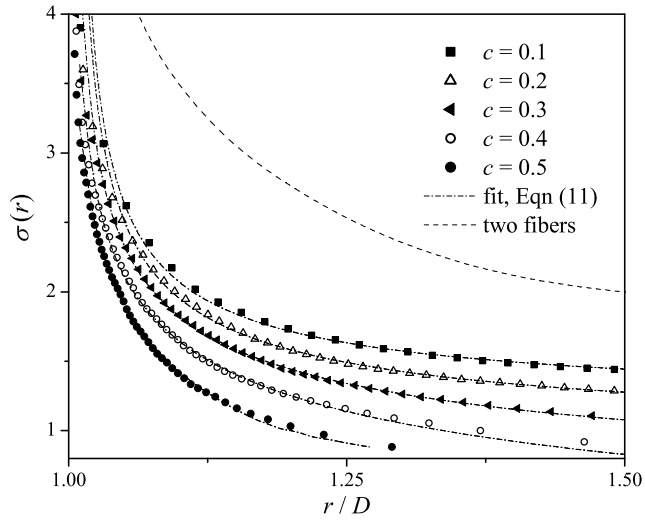


Figure 6. Peak interface stress versus interfiber distance: an effect of fiber volume content.

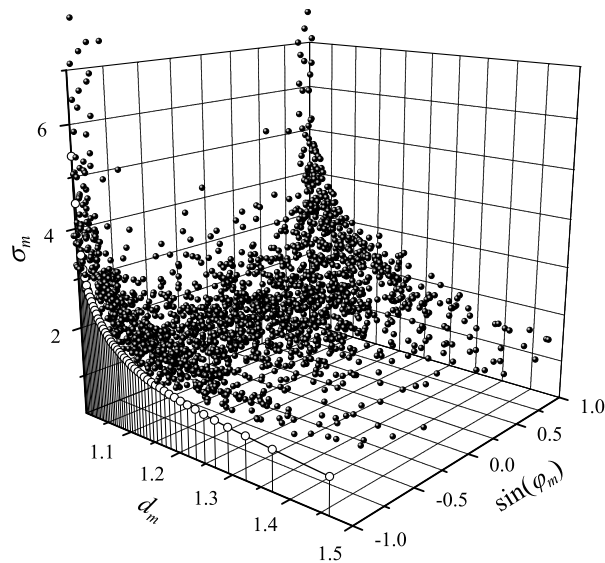


Figure 7. Peak interface stress versus nearest neighbor distance and orientation.

comparison, the corresponding curve $\sigma(r)$ taken from Figure 6 is shown in Figure 7 by the open circles. The conclusion can be made from this comparison that (11) gives a reasonable s_m approximation for φ_m close to $\pm\pi/2$ where the highest stress, and hence local damage, is expected.

Equation (11) is not perfect also in the sense that it does not work for $r = D$. The problem is that (6) allows for arbitrarily large stress and it results in singularity of (11) for touching fibers, which is not correct. This problem can be readily fixed by adding a small constant or c -dependent term to the expression in figure brackets. However, as seen from Figure 6, even in its present form it provides a rather good fit of the numerical data for, at least, $r/D \geq 1.02$.

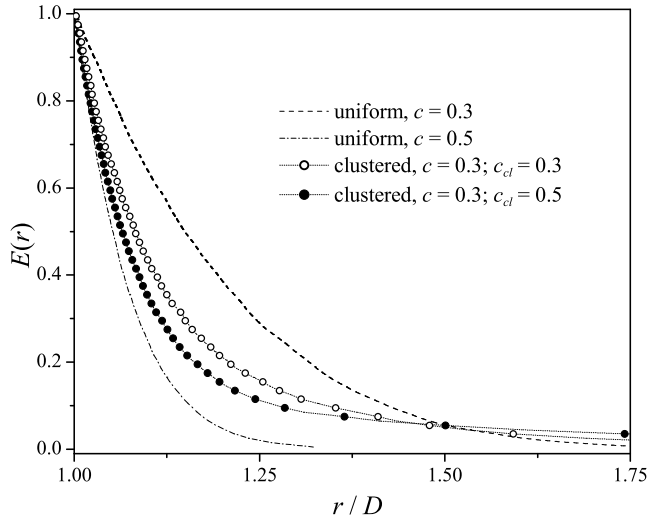


Figure 8. Exclusion probability function versus interfiber distance: an effect of cluster volume content.

4.3. Effect of clustering. Now, we consider local stress fields in FRCs containing fiber clusters of circular shape and estimate an effect of the cluster volume fraction c_{cl} . Specifically, we put the volume content of fibers in the cell and cluster $c = 0.3$ and $c_{in} = 0.5$, respectively. Obviously, $c = c_{in}c_{cl} + c_{out}(1 - c_{cl})$, where c_{out} is the fiber volume content outside the cluster: for the clusters with $c_{cl} = 0.3$ and $c_{cl} = 0.5$, we get $c_{out} = 0.21$ and $c_{out} = 0.10$, respectively.

An effect of clusters on the exclusion probability function is seen in [Figure 8](#), where the empirical function $\widehat{E}(r)$ obtained by computer simulation is shown by the solid and open circles. Here, for comparison's sake, we also plot $E(r)$ for FRC with uniform microstructure and $c = 0.3$ (dashed line) and $c = 0.5$ (dash-dotted line). As the comparison shows, it is rather sensitive to the nonuniformity in spatial distribution of fibers. Expectably, a clustered structure contains a larger number of closely placed fibers. As a result, the initial slope of $\widehat{E}(r)$ is close to that of a uniform structure with $c = 0.5$ rather than $c = 0.3$ (recall that the overall fiber volume content in a clustered FRC is 0.3).

In [Figure 9](#), the empirical probability function (4) $\widehat{F}(\sigma)$ is shown, calculated for the uniform and two clustered arrangements of fibers. The dash-dotted ($c_{cl} = 0.3$) and solid ($c_{cl} = 0.5$) curves deviate significantly from the dashed line representing the statistically uniform random structure. The data shown in [Figure 9](#) confirm the observation made of [[Pyrz 1994a](#)] that the mean value of maximal radial stress shifts markedly towards higher values for clustered patterns. It is noteworthy, however, that the empirical function $F_s(\sigma)$ built over the cluster area and shown by the solid and open triangles in [Figure 9](#) is statistically indistinguishable from that built over the whole cell area and shown in [Figure 9](#) by dash-dotted and solid lines. This means that clusterization increases the peak interface stress on the fibers inside and outside the cluster simultaneously.

By analogy with [Figure 6](#), one can match the numerical data in [Figures 8](#) and [9](#) to get $\sigma(r)$ for a clustered structure (see [Figure 10](#)). Here, the difference between the uniform and clustered structure is also quite observable. The “universal” $\sigma(r)$ curve, valid for any fiber arrangement type, is improbable: instead, one can rather expect it to be dependent on the parameters determining the nonuniform structure.

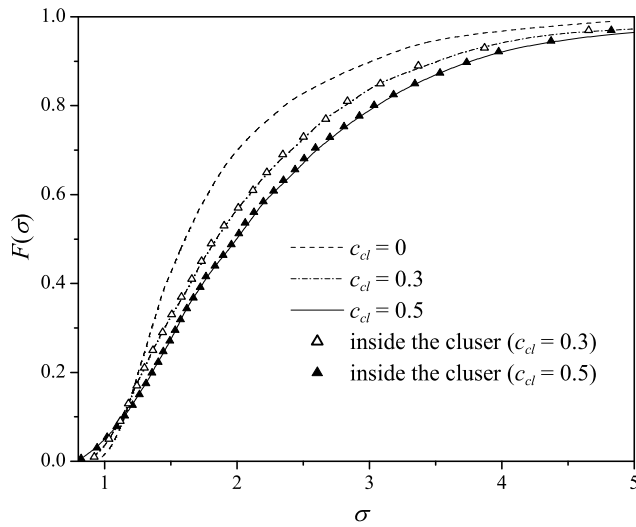


Figure 9. Peak interface stress distribution: an effect of the cluster volume content.

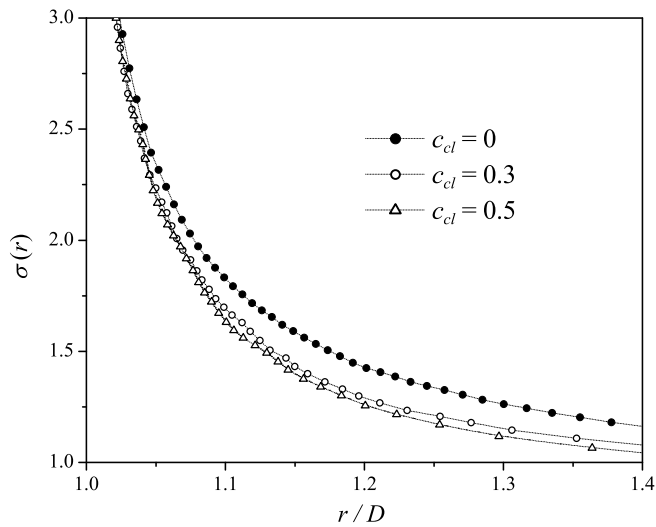


Figure 10. Peak interface stress versus interfiber distance: an effect of clusterization.

5. Microdamage model of FRC

The practical significance of the developed approach to studying the peak stress statistics is that it provides the theoretical background on which the micromechanics-based theories of FRC strength can be formulated. Below, we consider the simplest theory of this kind which, nevertheless, gives an idea of how available statistical information can be incorporated into the continuum damage model. Specifically, we assume that (a) the matrix-fiber interface is the “weakest link” in an FRC and that (b) debonding is

the only microdamage type. The damage criterion is taken in the form

$$\max_{0 \leq \varphi < 2\pi} \sigma_{rr} = \sigma_*,$$

where σ_* is the interface strength: $\sigma_* = \text{const}$ for brittle fracture and $\sigma_* = \sigma_*(N_c)$ for fatigue, N_c being a number of loading cycles. Alternatively, one can consider σ_* to be varying randomly from fiber to fiber, with a known statistical rule. An elementary damage event is the interface crack appearance, so it seems natural to consider the interface crack density as a damage parameter. Namely, $D = N_{db}/N_{\text{tot}}$, where N_{db} is a number of debonded fibers from a total number N_{tot} of fibers in the representative volume element of FRC.

Now, we recognize that N_{db} is a number of fibers with $s_m = \max \sigma_{rr}/P \geq \sigma_*/P$. Provided N_{tot} is taken to be sufficiently large,

$$D = N_{db}/N_{\text{tot}} = \Pr \{s_m \geq \sigma_*/P\} = 1 - F(\sigma_*/P), \quad (12)$$

where F is defined by (8). This formula gives an expression of damage level in terms of applied load $\sigma_{22}^* = P$ and interface strength σ_* . For example, assuming interface degradation due to cyclic loading, one can write the damage accumulation rule in an FRC as

$$D(N_c, \sigma_{22}^*, c) = 1 - \exp\left(-\left(\frac{p_3(c)}{\sigma_*(N_c)/P - p_1(c)}\right)^{p_2(c)}\right). \quad (13)$$

Note that (12) and (13) imply that D is sufficiently low and interactions between the cracks can be neglected. That is, this model can describe an early stage of interface damage development, characterized by rapid stiffness reduction (see, for example, [Brøndsted et al. 1997; van Paepegem and Degrieck 2002]). At low D , the effect of interface cracks on the effective elastic modulus E^* of FRC can be approximated by

$$E^*(D) = (1 - \beta D)E^*(0), \quad (14)$$

where β is a factor to be found experimentally or from simulation (see [Meraghni et al. 1996; Zhao and Weng 1997], among others). Together with (13), Equation (14) gives an estimate of stiffness reduction degree versus number of loading cycles. Predicted by our theory normalized effective Young modulus $E^*(D(N_c))/E^*(0)$ for the fiber volume content $c = 0.2, 0.3, 0.4$ and 0.5 is shown in Figure 11. Here, $\sigma_*(N_c) \sim N_c^{-1/m}$ is assumed for interface fatigue; also, we put $\beta = 1.85$ and $m = 3$. As seen from the plot, theory reproduces, at least, qualitatively, the experimental observations in [Brøndsted et al. 1997; van Paepegem and Degrieck 2002].

It would be naive to expect close quantitative correlation between this simple model and the fatigue behavior of real-life FRCs. For each specific composite material, there is a number of factors affecting substantially its strength but not taken into account in our theory. However, the considered model can readily be generalized in many ways, including loading type, interface debonding criterion, fatigue law, residual (setting) stress, etc. Incorporation of these (as well as other analogous) features makes the model more realistic: at the same time, it necessitates conducting a new series of numerical experiments by analogy with those described above. This work would be the subject of a separate paper: here, we emphasize only that the developed approach does not require introducing any simplifying assumptions regarding the stress fields. In contrast to most existing continuum theories of FRC microdamage (for

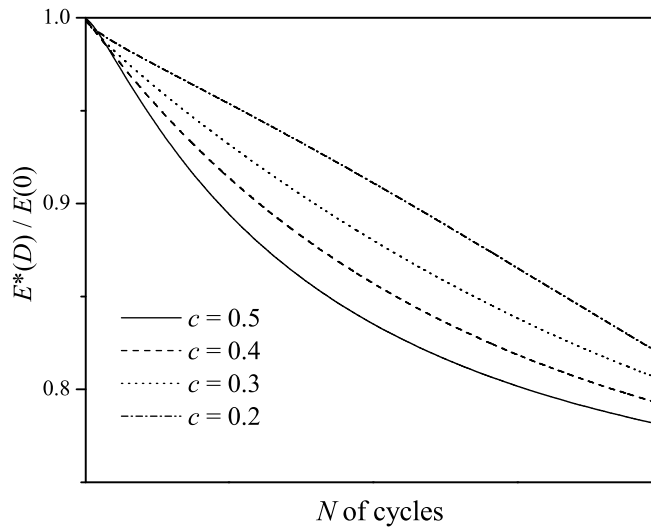


Figure 11. Stiffness reduction of an FRC due to cyclic loading.

their comprehensive review see, for example, [Degrieck and van Paepegem 2001]), we deal with the local, rather than phase-averaged, stress, which justifies application of the well-established strength criteria of phase materials and interfaces. Also, the proposed model provides a comprehensive account of microstructure and interactions between the fibers which cannot be expected in the theories based on the mean field or Eshelby-type models. Thus, the proposed approach captures the essential physical nature of the fatigue process and thus provides a reliable theoretical framework for a deeper insight into the fatigue damage initiation and accumulation phenomena in a fiber reinforced composite.

6. Conclusions

This paper addresses the effect of fiber arrangement and interactions on the peak interface stress statistics in a fiber reinforced material (FRC). The method we apply combines the multipole expansion technique with the representative unit cell model of random structure FRCs, capable of simulating both the uniform and clustered random fiber arrangements. By averaging over a number of numerical tests, the empirical probability functions have been obtained for the nearest neighbor distance and the peak interface stress. It is shown that the considered statistical parameters are rather sensitive to the fiber arrangement, particularly cluster formation. An explicit correspondence between them has been established and an analytical formula linking the microstructure and peak stress statistics in FRCs has been suggested. Application of the statistics of extremes to the local stress concentration study has been discussed. It is shown that the peak interface stress distribution in FRCs with uniform microstructure follows a Fréchet-type asymptotic distribution rule.

The presented numerical data demonstrate the potential of the developed approach: practical importance of the established relationships (as well as other analogous dependencies which can be obtained in this way) consists in the following. The ultimate goal of our simulations consists in development of the continuum theory of FRC strength. To accomplish this task, we need to link the microstructure parameters to the peak local stress statistics and microdamage initiation and accumulation rate. The

statistical parameters of an actual FRC microstructure and the constants entering the local stress distribution functions we found from the numerical experiments would be the input variables of this theory. As an example, a simple continuum model of interface damage accumulation in FRCs has been suggested based on the established in the work statistical distribution of peak interface stress.

Acknowledgements

The support by the Commission of the European Communities through the Sixth Framework Programme Grant UpWind.TTC (Contract #019945) is greatly acknowledged.

References

- [Babuška et al. 1999] I. Babuška, B. Andersson, P. J. Smith, and K. Levin, “[Damage analysis of fiber composites, I: Statistical analysis on fiber scale](#)”, *Comput. Methods Appl. Mech. Eng.* **172**:1–4 (1999), 27–77.
- [Beirlant et al. 2004] J. Beirlant, Y. Goegebeur, J. Segers, and J. Teugels, *Statistics of extremes: theory and applications*, Wiley, Chichester, 2004.
- [Beran 1968] M. J. Beran, *Statistical continuum theories*, Monographs in Statistical Physics and Thermodynamics **9**, Interscience, New York, 1968.
- [Bolotin 1988] V. V. Bolotin, *Prediction of service life for machines and structures*, ASME, New York, 1988.
- [Brøndsted et al. 1997] P. Brøndsted, H. Lilholt, and S. I. Andersen, “Fatigue damage prediction by measurements of the stiffness degradation in the polymer matrix composites”, pp. 370–377 in *International Conference on Fatigue of Composites: 8th International Spring Meeting* (Paris, 1997), edited by S. Degallaix et al., Soc. Française de Métallurgie et de Matériaux, Paris, 1997.
- [Buryachenko and Kushch 2006] V. A. Buryachenko and V. I. Kushch, “[Effective transverse elastic moduli of composites at non-dilute concentration of a random field of aligned fibers](#)”, *Z. Angew. Math. Phys.* **57**:3 (2006), 491–505.
- [Buryachenko et al. 2003] V. A. Buryachenko, N. J. Pagano, R. Y. Kim, and J. E. Spowart, “[Quantitative description and numerical simulation of random microstructures of composites and their effective elastic moduli](#)”, *Int. J. Solids Struct.* **40**:1 (2003), 47–72.
- [Byström 2003] J. Byström, “[Influence of the inclusions distribution on the effective properties of heterogeneous media](#)”, *Compos. B Eng.* **34**:7 (2003), 587–592.
- [Chen and Papathanasiou 2004] X. Chen and T. D. Papathanasiou, “[Interface stress distributions in transversely loaded continuous fiber composites: parallel computation in multi-fiber RVEs using the boundary element method](#)”, *Compos. Sci. Technol.* **64**:9 (2004), 1101–1114.
- [Degrieck and van Paeppegem 2001] J. Degrieck and W. van Paeppegem, “[Fatigue damage modeling of fibre-reinforced composite materials: review](#)”, *Appl. Mech. Rev. (ASME)* **54**:4 (2001), 279–300.
- [Drago and Pindera 2007] A. Drago and M.-J. Pindera, “[Micro-macromechanical analysis of heterogeneous materials: macroscopically homogeneous vs periodic microstructures](#)”, *Compos. Sci. Technol.* **67**:6 (2007), 1243–1263.
- [Fisher and Tippett 1928] R. A. Fisher and L. H. C. Tippett, “[Limiting forms of the frequency distribution of the largest or smallest member of a sample](#)”, *Math. Proc. Cambridge Philos. Soc.* **24**:2 (1928), 180–190.
- [Foster et al. 2006] D. C. Foster, G. P. Tandon, and M. Zoghi, “[Evaluation of failure behavior of transversely loaded unidirectional model composites](#)”, *Exp. Mech.* **46**:2 (2006), 217–243.
- [Frayssé et al. 1998] V. Frayssé, L. Giraud, and G. S., “A set of flexible-GMRES routines for real and complex arithmetics”, Technical Report TR/PA/98/20, CERFACS, 1998.
- [Freudenthal 1968] A. M. Freudenthal, “Statistical approach to brittle fracture”, Chapter 6, pp. 591–619 in *Fracture, an advanced treatise, 2: Mathematical fundamentals*, edited by H. Liebowitz, Academic Press, New York, 1968.
- [Ganguly and Poole 2004] P. Ganguly and W. J. Poole, “[Influence of reinforcement arrangement on the local reinforcement stresses in composite materials](#)”, *J. Mech. Phys. Solids* **52**:6 (2004), 1355–1377.

- [Gnedenko 1943] B. V. Gnedenko, “Sur la distribution limite du terme maximum d’une série aléatoire”, *Ann. Math.* **44**:3 (1943), 423–453.
- [Golovchan et al. 1993] V. T. Golovchan, A. N. Guz, Y. Kohanenko, and V. I. Kushch, *Statics of materials*, Mechanics of Composites **1**, Naukova Dumka, Kiev, 1993.
- [Greengard and Helsing 1998] L. Greengard and J. Helsing, “On the numerical evaluation of elastostatic fields in locally isotropic two-dimensional composites”, *J. Mech. Phys. Solids* **46**:8 (1998), 1441–1462.
- [Gumbel 1958] E. J. Gumbel, *Statistics of extremes*, Columbia University Press, New York, 1958.
- [Kushch et al. 2008] V. I. Kushch, S. V. Shmegeera, and L. Mishnaevsky, Jr., “Meso cell model of fiber reinforced composite: interface stress statistics and debonding paths”, *Int. J. Solids Struct.* **45**:9 (2008), 2758–2784.
- [Meraghni et al. 1996] F. Meraghni, C. J. Blakeman, and M. L. Benzeggagh, “Effect of interfacial decohesion on stiffness reduction in a random discontinuous-fibre composite containing matrix microcracks”, *Compos. Sci. Technol.* **56**:5 (1996), 541–555.
- [Meraghni et al. 2002] F. Meraghni, F. Desrumaux, and M. L. Benzeggagh, “Implementation of a constitutive micromechanical model for damage analysis in glass mat reinforced composite structures”, *Compos. Sci. Technol.* **62**:16 (2002), 2087–2097.
- [Mishnaevsky 2007] L. Mishnaevsky, Jr., *Computational mesomechanics of composites: numerical analysis of the effect of microstructures of composites on their strength and damage resistance*, Wiley, Chichester, 2007.
- [van Paepegem and Degrieck 2002] W. van Paepegem and J. Degrieck, “A new coupled approach of residual stiffness and strength for fatigue of fibre-reinforced composites”, *Int. J. Fatigue* **24**:7 (2002), 747–762.
- [Pyrz 1994a] R. Pyrz, “Correlation of microstructure variability and local stress field in two-phase materials”, *Mater. Sci. Eng. A* **177**:1–2 (1994), 253–259.
- [Pyrz 1994b] R. Pyrz, “Quantitative description of the microstructure of composites, 1: Morphology of unidirectional composite systems”, *Compos. Sci. Technol.* **50**:2 (1994), 197–208.
- [Pyrz and Bochenek 1998] R. Pyrz and B. Bochenek, “Topological disorder of microstructure and its relation to the stress field”, *Int. J. Solids Struct.* **35**:19 (1998), 2413–2427.
- [Saad and Schultz 1986] Y. Saad and M. H. Schultz, “GMRES: a generalized minimal residual algorithm for solving nonsymmetric linear systems”, *SIAM J. Sci. Stat. Comput.* **7**:3 (1986), 856–869.
- [Torquato 1995] S. Torquato, “Nearest-neighbor statistics for packings of hard spheres and disks”, *Phys. Rev. E* **51**:4 (1995), 3170–3182.
- [Torquato 2002] S. Torquato, *Random heterogeneous materials: microstructure and macroscopic properties*, Springer, New York, 2002.
- [Wang et al. 2005] J. Wang, S. L. Crouch, and S. G. Mogilevskaya, “A fast and accurate algorithm for a Galerkin boundary integral method”, *Comput. Mech.* **37**:1 (2005), 96–109.
- [Zhao and Weng 1997] Y. H. Zhao and G. J. Weng, “Transversely isotropic moduli of two partially debonded composites”, *Int. J. Solids Struct.* **34**:4 (1997), 493–507.

Received 24 Nov 2008. Revised 7 Apr 2009. Accepted 19 Jun 2009.

VOLODYMYR I. KUSHCH: vkushch@bigmir.net

National Academy of Sciences of Ukraine, Institute for Superhard Materials, 2 Avtozavodskaya St., Kiev 04074, Ukraine

SERGIY V. SHMEGERA: ssmegeera@bigmir.net

National Academy of Sciences of Ukraine, Institute for Superhard Materials, 2 Avtozavodskaya St., Kiev 04074, Ukraine

LEON MISHNAEVSKY JR.: leon.mishnaevsky@risoe.dk

Technical University of Denmark, Risø National Laboratory for Sustainable Energy, Frederiksborgvej 399, 4000 Roskilde, Denmark